Available online at www.sciencedirect.com
ScienceDirect
Thermochimica Acta 467 (2008) 1–10
thermochimica acta
www.elsevier.com/locate/tca

Kinetic analysis of the oxidative decomposition in γ-zirconium and γ-titanium phosphate intercalation compounds The case of 2,2′-bipyridyl and its copper complex formed *in situ*

Stefano Vecchio [a,*], Romolo Di Rocco [b], Carla Ferragina [b]

[a] *Department of Chemical Engineering (I.C.M.A), University of Rome "La Sapienza", via del Castro Laurenziano 7, 00161 Rome, Italy*

[b] *CNR, Istituto di Metodologie Inorganiche e dei Plasmi, via Salaria km. 29.300, 00016 Monterotondo, Rome, Italy*

Received 18 November 2006; received in revised form 25 October 2007; accepted 25 October 2007
Available online 4 November 2007

Abstract

The thermal behaviour of the heterocyclic compound 2,2′-bipyridyl and its copper complex formed *in situ*, both intercalated between the layers of γ-zirconium and γ-titanium phosphates was studied by simultaneous thermogravimetry and differential scanning calorimetry techniques using non-isothermal constant heating rate conditions up to 873 K under a stream of air. In all the obtained intercalation materials, which are found to be stable up to 600 K, the ligand shows an oxidative decomposition practically in only one step. Model-free isoconversional method of Ozawa–Flynn–Wall, applied to the vaporization of pure 2,2′-bipyridyl and to the oxidative decomposition step occurring in each intercalation material examined, yields practically constant activation energies for values of the fraction decomposed $\alpha \leq 0.7$. The activation energies calculated using the best fit between calculated and theoretical $g(\alpha)$ models do not differ significantly from the corresponding mean E values selected using the isoconversional OFW method in the range $\alpha \leq 0.7$. Activation energies derived by the Kissinger method show a good agreement with the mean values derived by the former method, and the Arrhenius rate constants determined using also the pre-exponential factor values enable to conclude that the bipyCu intercalation materials show a destabilizing effect with respect to the corresponding bipy intercalation materials (negligible difference in the oxidative decomposition temperatures, but a significant difference in the rate constant values: at least one order of magnitude).

Keywords: Ion-exchangers; Intercalation compounds; TG; DSC; Ozawa–Flynn–Wall method; Kissinger method; Coats–Redfern method

1. Introduction

Acid phosphates of tetravalent metals such as Zr, Ti and Sn are insoluble ion-exchangers that can be prepared in crystalline forms with nonrigid layered structures. The most studied among these materials, γ-zirconium and γ-titanium phosphates (γ-ZrP, γ-TiP) [1–3], are well known to exchange metal ions [4,5], to intercalate organic bases [6,7] and to support non-polar molecules [8,9]. The intercalation compounds that were obtained by intercalating polar organic bases easily exchange transition metal ions that are subsequently coordinated to the base through the layers, giving rise to complexes formed *in situ* between the layers of the host matrices. In the present study, as a follow-up of our previous studies [10,11], γ-ZrP and γ-TiP were intercalated with the organic base 2,2′-bipyridyl (bipy) and denoted as γ-ZrPbipy, γ-TiPbipy. The two obtained materials were subsequently exchanged with copper ions to give complex formed *in situ* (γ-ZrPbipyCu, γ-TiPbipyCu). These materials were prepared with a particular view to obtain either catalysts or catalyst precursors to be used in heterogeneous catalysis by complexes usually utilized in the homogeneous catalysis [12–14]. The present study is devoted to characterize the thermal oxidative decomposition of these intercalation materials using different kinetic methods and provide reliable Arrhenius parameters and a suitable model function for each process studied. On the other hand, to the best of our knowledge, no relevant information are available in literature on the oxidative decomposition kinetics of bipy not intercalated or intercalated (as such or as a copper complex) between the layers of these ion-exchangers.

* Corresponding author. Tel.: +39 06 4976 6906; fax: +39 06 4976 6749.
E-mail address: stefano.vecchio@uniroma1.it (S. Vecchio).

0040-6031/$ – see front matter © 2007 Elsevier B.V. All rights reserved.
doi:10.1016/j.tca.2007.10.015

2. Experimental and method

2.1. Chemicals

The copper acetate, zirconyl chloride, titanium oxide, phosphoric acid and 2,2′-bipyridyl were supplied by Aldrich (reagent grade) and used without further purification.

2.2. Materials

The precursors (γ-ZrP and γ-TiP), the intercalation compounds obtained with bipy (γ-ZrPbipy and γ-TiPbipy) and the copper complexes formed *in situ* (γ-ZrPbipyCu and γ-TiPbipyCu) were prepared as reported in literatures ([2,3] and [15,16], respectively). Intercalation of bipy and formation of the bipyCu complex between the layers of the exchangers evidenced by X-ray photoelectron spectroscopic measurements in [17] are outlined in Fig. 1 for γ-ZrP as an example.

2.3. Physical measurements and chemical analysis

Copper ions were determined in the supernatant solutions, before and after contact with the exchangers with a GBC 903 A.A. spectrophotometer. Phosphates were determined colorimetrically [18]. X-ray powder diffraction (XRPD) was used to study phase changes in the materials by monitoring the reflection and its armonics. A Philips diffractometer (model PW 1130/00) was used with Ni-filtered Cu Kα radiation (λ = 1.541 Å).

2.4. Thermal measurements

Water and the bipy contents and the thermal behaviour of the tested materials as well as of pure bipy were determined with a simultaneous TG/DTA Stanton Redcroft 1500 thermoanalyzer, Pt crucibles, heating rate 10 K min^{-1} calcined up to 1373 K to constant weight in an airflow. The TG and DSC experimental measurements were carried out on a simultaneous Stanton Redcroft 625 thermoanalyzer, connected to 386 IBM-compatible personal computer. Thermodynamic quantities were calculated using the Stanton Redcroft Data Acquisition System, Trace 2, version 4. Temperature and heat flow rate scales were calibrated with very pure standards (indium, lead, tin, zinc), whose melting temperatures and enthalpies are well known [19]. Samples of 6–8 mg were weighed into Al pans in an argon-filled dry box to avoid a possible sample degradation, and then in the thermoanalyzer, where the purge air stream fluxed to continuously remove the gases given off during the thermal heating process experiment. As far as the thermal analysis study is concerned, three TG/DSC experiments were made for each material at 8 K min^{-1} using fresh samples only and a good precision of experimental data was obtained (<1%). On the other hand, for the kinetic analysis the TG/DSC measurements have been carried out at different heating rates (2, 4, 6 and 8 K min^{-1}) up to 873 K under a 100 ml min^{-1} stream of air.

3. Theory

Kinetics of solid-state reactions is usually described by the following basic equation:

$$\frac{d\alpha}{dt} = k(T) f(\alpha) \tag{1}$$

where α is the fraction decomposed defined as $\alpha = (1/Q_{tot}) \int_0^f (dQ/dt)dt$ (being Q_{tot} and dQ/dt the overall heat of reaction and the heat flux, respectively), $f(\alpha)$ the model function, which assumes different mathematical forms depending on the reaction mechanism [20] and $k(T)$ is the specific rate constant, whose temperature dependence is commonly described by the Arrhenius equation:

$$k(T) = A \exp\left(-\frac{E}{RT}\right) \tag{2}$$

where E is the activation energy, A the pre-exponential factor, R the gas constant and T is the absolute temperature. Moreover, taking into account that under non-isothermal condition the heating rate $\beta = dT/dt$, where t is the time, by combining Eqs. (1) and (2), it results

$$\frac{d\alpha}{dT} = \frac{d\alpha}{dt}\frac{dt}{dT} = \left(\frac{A}{\beta}\right) \exp\left(-\frac{E}{RT}\right) f(\alpha) \tag{3}$$

Most of the methods that describe the kinetics of reactions in solids use Eq. (3) as well as several approximation of its integral

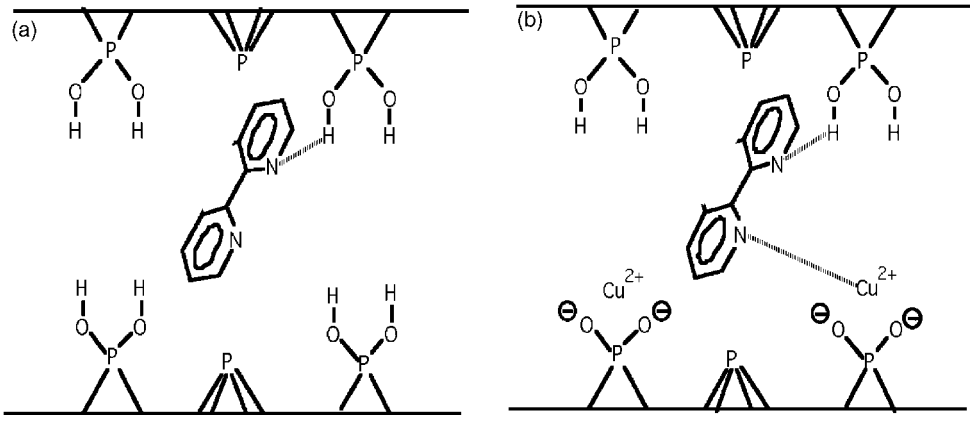

Fig. 1. Possible arrangements of bipy (a) and bipyCu complex (b) between the layers of the γ-ZrP exchanger.

Table 1
Most commonly used differential and integral model functions to describe the thermal oxidative decomposition processes

N	Model function	$f(\alpha)$	$g(\alpha) = kt$
1	Power law	$4(\alpha)^{3/4}$	$(\alpha)^{1/4}$
2	Power law	$3(\alpha)^{2/3}$	$(\alpha)^{1/3}$
3	Power law	$2(\alpha)^{1/2}$	$(\alpha)^{1/2}$
4	Power law	$2/3(\alpha)^{-1/2}$	$(\alpha)^{3/2}$
5	One-dimensional diffusion	$1/(2\alpha)$	$(\alpha)^2$
6	Mampel (first-order)	$1-\alpha$	$-\ln(1-\alpha)$
7	Avrami-Erofeev	$4(1-\alpha)[-\ln(1-\alpha)]^{3/4}$	$[-\ln(1-\alpha)]^{1/4}$
8	Avrami-Erofeev	$3(1-\alpha)[-\ln(1-\alpha)]^{2/3}$	$[-\ln(1-\alpha)]^{1/3}$
9	Avrami-Erofeev	$2(1-\alpha)[-\ln(1-\alpha)]^{1/2}$	$[-\ln(1-\alpha)]^{1/2}$
10	Three-dimensional diffusion	$3/2(1-\alpha)^{2/3}[1-(1-\alpha)^{1/3}]^{-1}$	$[1-(1-\alpha)^{1/3}]^2$
11	Contracting sphere	$3(1-\alpha)^{2/3}$	$1-(1-\alpha)^{1/3}$
12	Contracting cylinder	$2(1-\alpha)^{1/2}$	$1-(1-\alpha)^{1/2}$
13	Zero-order	1	α
14	Second-order	$(1-\alpha)^2$	$(1-\alpha)^{-1}-1$

form

$$g(\alpha) = \left(\frac{A}{\beta}\right)\int_0^T \exp\left(-\frac{E}{RT}\right)\mathrm{d}T \tag{4}$$

where

$$g(\alpha) = \int_0^\alpha (f(\alpha))^{-1}\mathrm{d}\alpha \tag{5}$$

is the integral form of the model function that does not depend on the heating rate used.

3.1. Model-free methods

However, due to the complexity of the kinetic description concerning the solid-state decomposition processes it is usually assumed that the activation energy is not a constant value but depends on α [21,22]. Therefore, in order to establish if such dependence exists or not, the kinetic procedure adopted in this work was first based on two multi-heating rate methods. Both approaches determine the activation energy using thermal analysis data carried out at different fixed heating rates without choosing a priori a defined model function. In particular, the first kinetic method used was the isoconversional method of Ozawa–Flynn–Wall (OFW) [23,24] that is based on the integral form of Eq. (1) according to the following isoconversional equations:

$$\ln(\beta)_\alpha = \ln\left[\frac{A_\alpha E_\alpha}{R}\right] - \ln g(\alpha) - 5.3305 - 1.052\left(\frac{E_\alpha}{R}\right)\left(\frac{1}{T_\alpha}\right) \tag{6}$$

Once the Doyle's approximation [25]: $\ln p(x) = -5.3305 - 1.052x$, where $x = E_\alpha/(RT_\alpha)$ and $20 \le x \le 60$) is verified to be valid over the entire range of α, then at any selected value of α, from the slope of the related regression straight line derived by the $\ln(\beta)_\alpha$ vs. $1/T_\alpha$ plot, the corresponding E_α value is derived as a function of α. The present kinetic study was also performed using the Kissinger method [26] that uses the following equation:

$$\ln\left(\frac{\beta}{T_\mathrm{m}^2}\right) = \ln\left[\frac{AR}{E}\right] + \left(-\frac{E}{R}\right)\left(\frac{1}{T_\mathrm{m}}\right) \tag{7}$$

where T_m is the DSC peak temperature at a given heating rate β. From the slope of Eq. (7) a single activation energy value for each step of mass loss is given.

3.2. Model-fitting methods

In a usual model-fitting procedure particular differential or integral model functions $f(\alpha)$ or $g(\alpha)$, respectively (Table 1), assumed to solve Eq. (3) or Eq. (4), and determine the Arrhenius parameters by fitting the kinetic equation to the experimental data. However, Vyazovkin and Wight [27] revealed that this approach usually gives unreliable results for two kinds of reasons. In fact, the model-fitting method is unable to show the variation of the activation energy with the extent of reaction that is generally observed especially in multi-step processes. Furthermore, it is difficult to select among the different model functions on the basis of the best fit to the experimental data. To overcome this difficulty, we have previously verified that both the E and A values practically do not depend on α by using the above-mentioned isoconversional OFW method. Subsequently, TG data derived by a single linear heating rate experiment were fitted to some of the integral model functions $g(\alpha)$ reported in literature [27] using the Coats–Redfern (CR) method [28]. This method makes the assumption that the integral model function

$$\ln\left[\frac{g_j(\alpha)}{T^2}\right] = \ln\left\{\left[\frac{A_j R}{\beta E}\right]\left[1-\left(\frac{2R\langle T\rangle}{E_j}\right)\right]\right\} - \frac{E_j}{RT} \tag{8}$$

where the subscript j is related to the selected reaction model and $\langle T\rangle$ is the average of the experimental temperature range. Each $g_j(\alpha)$ expression in Table 1 is inserted in Eq. (8) and from the slope of the linear regression obtained by plotting $\ln[g_j(\alpha)/T^2]$ against $1/T$ the corresponding Arrhenius parameters E_j and A_j are obtained for each model function j. These Arrhenius parameters related to all the different model function j of the same

process are linearly correlated (compensation effect). The linear regression parameters obtained were used to estimate the isoconversional $\ln A_\alpha$ value at each given conversion by replacing the E_j values with the isoconversional E_α ones in the regression equation [22].

3.3. Reconstruction of the reaction models of the processes examined

OFW, Kissinger and CR methods do not enable the pre-exponential factor and the model function of the process examined to be suitably analyzed. On the other hand, the integrated model function $g(\alpha)$ can be numerically reconstructed using an artificial isokinetic relationship [22,29] if E_α were practically independent of α. Once the values of $\ln A_\alpha$ and E_α are determined the integrated model function $g(\alpha)$ is reconstructed by substituting the selected estimates of A_α and E_α in Eq. (4). The explicit form of the model function can be determined by comparing the selected numerical dependence of $g(\alpha)$ vs. α with the model dependencies displayed in Table 1.

4. Results and discussion

4.1. Materials

The proposed chemical formulas along with their interlayer distances d are summarized in Table 2. As it can be seen the amount of bipy in γ-ZrPbipyCu and γ-TiPbipyCu is lower than that of γ-ZrPbipy and γ-TiPbipy materials. This is ascribed to the small elution of bipy noticed after the formation of the Cu complex in both the exchangers due to the steric hindrance occurring during the Cu^{2+} exchange [30].

4.2. XRPD

From the XRPD patterns of the intercalation materials at room temperature an appreciable increase of the d (about 1.55 and 2.75 Å) is observed when bipy is intercalated between the layers of the two considered exchangers compared to those of their precursors γ-ZrP and γ-TiP (Table 2). The d in γ-ZrPbipyCu is appreciably higher (16.96 Å) than that of γ-ZrPbipy (13.85 Å). By contrast, identical d values are found in γ-TiPbipy and γ-TiPbipyCu. It is worth noting that the complex formation not always occurs with an increase of the d.

Table 2
Chemical composition and interlayer distances d of the examined materials

Materials		d (Å)
γ-ZrP	γ-$Zr(PO_4)(H_2PO_4)\cdot 2H_2O$	12.30
γ-ZrPbipy	γ-$Zr(PO_4)(H_2PO_4)$ $bipy_{0.48}\cdot 0.30H_2O$	13.85
γ-ZrPbipyCu	γ-$Zr(PO_4)(H_{1.20}PO_4)Cu_{0.40}bipy_{0.43}\cdot 0.40H_2O$	16.96
γ-TiP	γ-$Ti(PO_4)(H_2PO_4)\cdot 2H_2O$	11.60
γ-TiPbipy	γ-$Ti(PO_4)(H_2PO_4)$ $bipy_{0.43}\cdot 0.40H_2O$	14.35
γ-TiPbipyCu	γ-$Ti(PO_4)(H_{1.24}PO_4)Cu_{0.38}bipy_{0.40}\cdot 0.38H_2O$	14.35

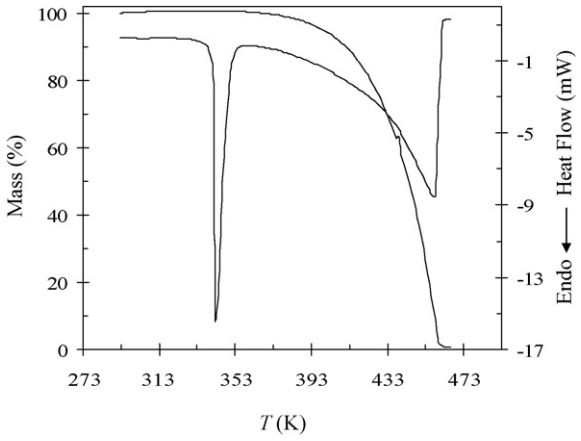

Fig. 2. TG and DSC curves of pure bipy at 8 K min^{-1} under a stream of air.

Table 3
Melting and vaporization enthalpies of bipy at different heating rates

β (K min^{-1})	ΔH_{fus} (kJ mol^{-1})	ΔH_{vap} (kJ mol^{-1})
2	17.6 ± 0.7	58.6 ± 2.0
4	17.5 ± 0.6	59.0 ± 2.3
6	17.6 ± 0.8	58.8 ± 2.4
8	17.4 ± 0.7	58.4 ± 2.4

4.3. Thermal and kinetic analysis

4.3.1. 2,2′-Bipyridyl

The TG and DSC curves of pure bipy are shown in Fig. 2. After melting at about 343 K a single step of mass loss is shown, accompanied by an asymmetric endothermic DSC peak ascribed to vaporization. From the area of the DSC peaks obtained by carrying out experiments at different heating rates the corresponding ΔH_{fus} and ΔH_{vap} values of pure bipy are selected and given in Table 3. No actual dependence of ΔH_{fus} and ΔH_{vap} values on β can be observed.

The dependence of E values on α for vaporization of pure bipy is displayed in Fig. 3. Practically constant E values around 61 ± 2 kJ mol^{-1} were found (changes lie within the associated uncertainties). According to these results, the x values ($x = E/RT$) are slightly higher than 20, which is the lower limit to apply the

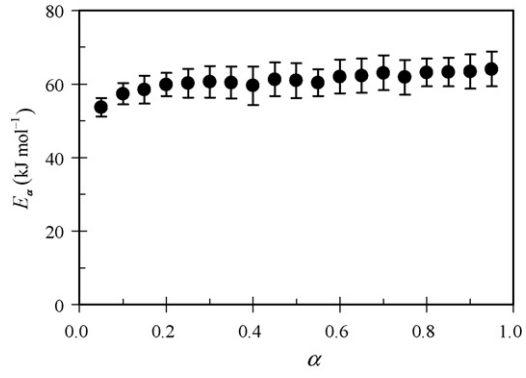

Fig. 3. Dependency of the activation energy on α (OFW method) for the vaporization process of pure bipy.

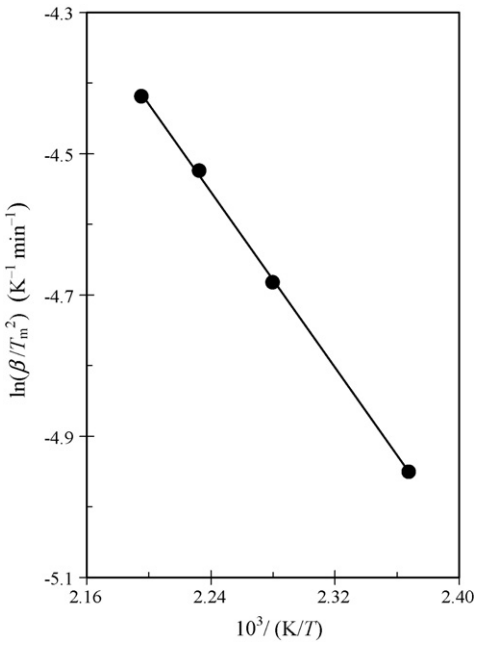

Fig. 4. Kissinger plot for the vaporization process of pure bipy.

Doyle's approximation. On the other hand, from the slope of the regression line obtained by fitting the $\ln(\beta/T_m^2)$ experimental data against T_m^{-1} (Fig. 4) according to Eq. (7), the activation energy of vaporization for pure bipy equal to 54 ± 3 kJ mol^{-1} is found. The result obtained is very close to the average vaporization enthalpy (Table 3). In addition, a good agreement is found between the activation energies derived from OFW method and the E value derived by the Kissinger method. The Arrhenius parameters for vaporization of pure bipy are also determined by the CR model-fitting method for all the model functions of Table 1 and given in Table 4 with their R^2 values. A single function cannot be discriminated since the four power law, one- and three-dimensional diffusion, contracting and zero-order models seem to be statistically equivalent fitting models. On the other hand, Fig. 5 shows a comparison of $g(\alpha)$ derived from

Table 4
Arrhenius parameters related to vaporization of pure bipy at 8 K min^{-1} obtained by the Coats–Redfern method for the most commonly used model functions

N	E (kJ mol^{-1})	ln A (min^{-1})	R^2
1	11.6	1.1	0.9962[a]
2	17.9	2.7	0.9974[a]
3	30.4	6.2	0.9981[a]
4	105.5	26.9	0.9988[a]
5	143.0	37.0	0.9988[a]
6	87.4	22.6	0.9893
7	16.5	2.5	0.9827
8	24.4	4.7	0.9856
9	40.1	9.3	0.9877
10	42.9	9.8	0.9984[a]
11	17.9	2.7	0.9974[a]
12	77.0	18.8	0.9981[a]
13	67.7	16.7	0.9986[a]
14	112.5	30.1	0.9520

[a] Statistically equivalent models.

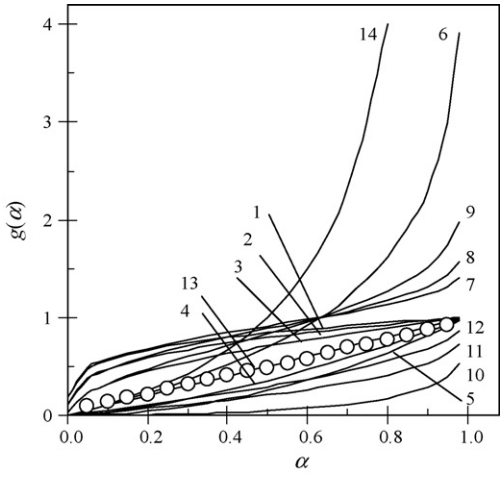

Fig. 5. Conversion dependence of $g(\alpha)$ for the model functions listed in Table 1 (—) and for the experimental data (◯) related to vaporization of pure bipy.

experimental vaporization data (using Eq. (4)) with the model functions reported in Table 1. The closest match over the entire range of conversion is fulfilled by the zero-order function. This result was already found by other authors in their studies on vaporization without decomposition [31–33]. Moreover, as a further confirmation of the reliability of the result obtained the associated E value in Table 4 is in excellent agreement with the mean isoconversional E value.

4.3.2. Intercalation materials

On the other hand, the TG and DSC curves of the intercalation materials are given in Fig. 6. It is evident that their thermal behaviour is quite different from that of pure bipy. In fact, in all four examined intercalated materials noticeable exothermic effects ascribed to oxidative decomposition of bipy occur from 550 to 873 K after more or less evident dehydration processes. All four intercalated materials show the ligand oxidative decomposition occurring in only one step between 650 and 873 K, accompanied by a very intense exothermic effect shown in the DSC curves.

Our attention was then focused on the kinetic study of the oxidative decomposition process by applying the OFW and Kissinger methods. As far as the results of the OFW method is concerned, the E_α values were determined from the slopes of the $(\ln \beta)_\alpha$ vs. $1/T_\alpha$ linear equations and presented in terms of the conversion dependence of the activation energy in Fig. 7. Activation energies practically independent of the fraction decomposed α were found in the range $\alpha \leq 0.7$. In spite of the complex nature usually shown in oxidative decomposition processes an increasing trend of E values was observed only in the range $\alpha > 0.70$ for the intercalated bipy materials, while for the bipyCu materials E practically does not change over the entire range of α. These results suggest that, contrary to what it could be expected, the main part of the reaction has a single-step nature describable by a single reaction mechanism.

For comparison purposes, the E and ln A values of the oxidative decomposition for the intercalation compounds were also calculated using the Kissinger method from the slope and

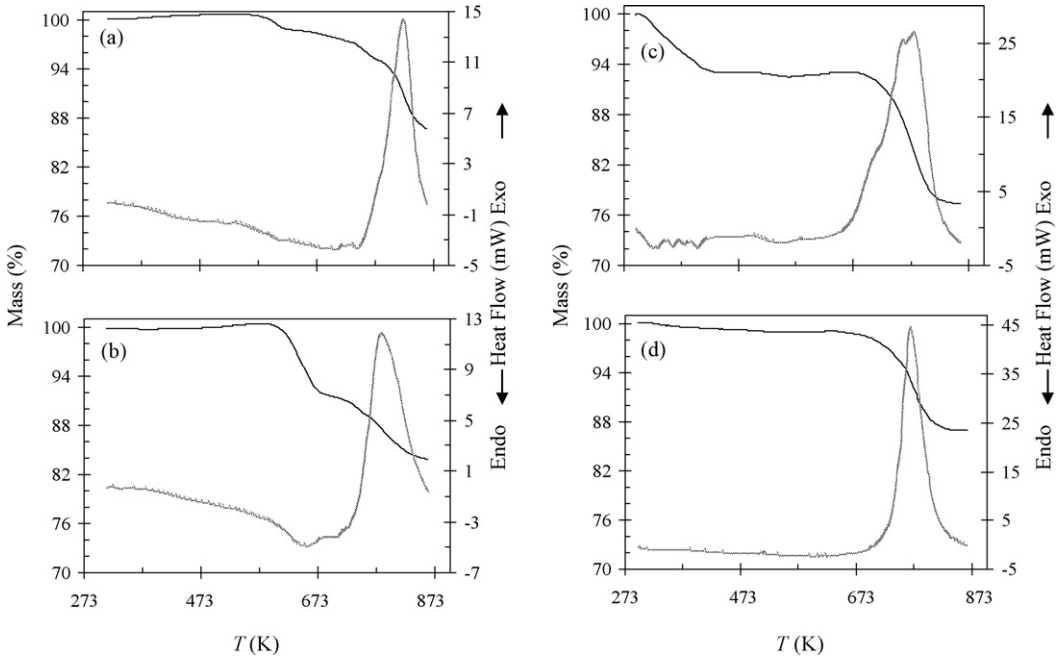

Fig. 6. TG and DSC curves at 8 K min^{-1} under a stream of air for (a) γ-ZrPbipy, (b) γ-ZrPbipyCu, (c) γ-TiPbipy and (d) γ-TiPbipyCu.

intercept of the $\ln(\beta/T_m^2)$ vs. T_m^{-1} regression line (Eq. (7)), respectively (Fig. 9). On the other hand, in order to better individuate the T_m values the DSC curves at different heating rates were reported in Fig. 8 for all the intercalation materials investigated. The derived regression and kinetic parameters are reported in Table 5. The average E values selected with the OFW method (even if actually slightly higher) agree quite well with those of the Kissinger one within the associated experimental errors. In addition, because of the negligible dependence of E on the degree of conversion α for the oxidative decomposition process of all the intercalated materials examined in the range $\alpha \leq 0.7$, the most suitable model functions were selected from the best agreement between the $g(\alpha)$ values determined by Eq. (4) with those calculated using the expressions in Table 1. If the comparison is suitably restricted in the range $\alpha \leq 0.7$, a reasonable agreement with a single model is found for the oxidative decomposition of each intercalation compound even if some deviations are still observed in the range $\alpha > 0.8$. Fig. 10 shows that for the

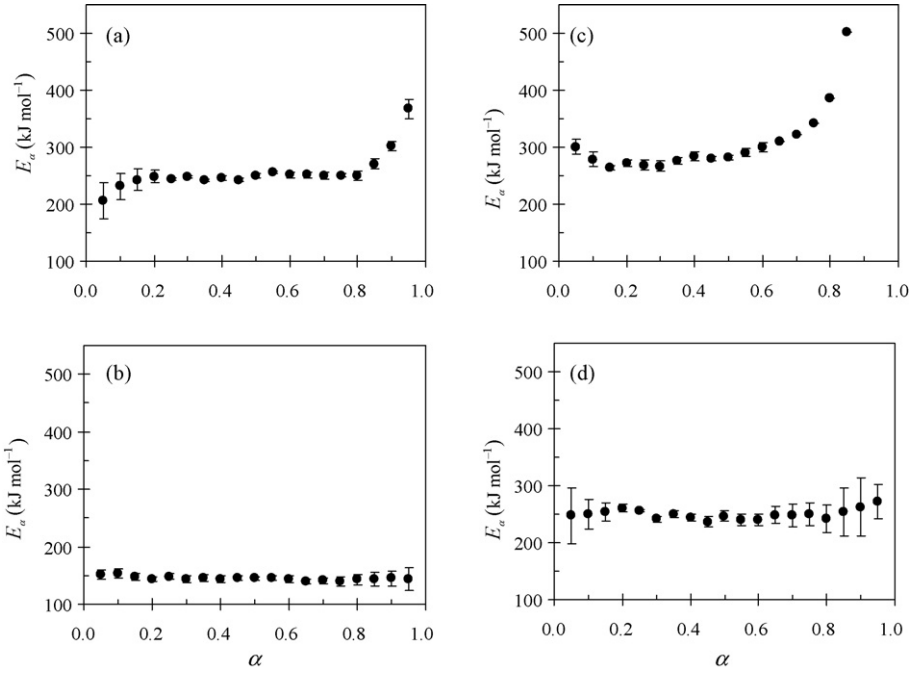

Fig. 7. Dependency of the activation energy on α (OFW method) for the oxidative decomposition process in (a) γ-ZrPbipy, (b) γ-ZrPbipyCu, (c) γ-TiPbipy and (d) γ-TiPbipyCu.

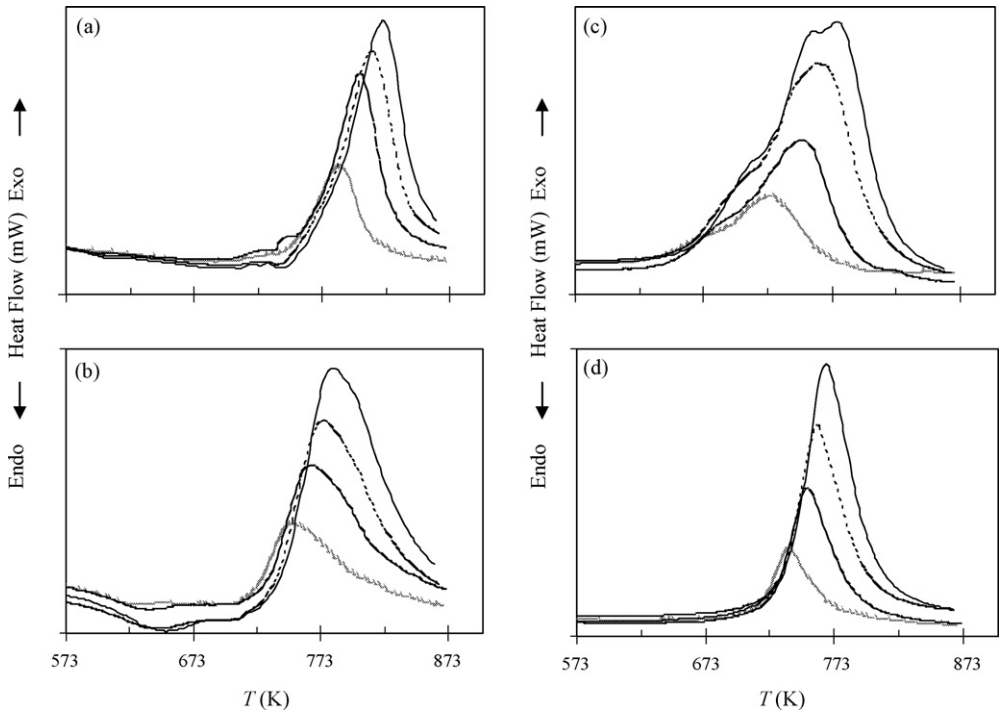

Fig. 8. DSC curves at 2, 4, 6 and 8 K min^{-1} under a stream of air for (a) γ-ZrPbipy, (b) γ-ZrPbipyCu, (c) γ-TiPbipy and (d) γ-TiPbipyCu.

Table 5
Regression and Arrhenius parameters for the oxidative decomposition process by the Kissinger method

Materials	$\ln(\beta/T_m^2) = a + b(10^3/T_m)$		R^2	E (kJ mol^{-1})	$\ln A$ (min^{-1})
	a	b			
γ-ZrPbipy	8.1 ± 0.7	−10.7 ± 0.6	0.9941	194 ± 11	18.1 ± 1.0
γ-ZrPbipyCu	4.6 ± 0.7	−7.3 ± 0.3	0.9961	133 ± 6	14.3 ± 0.6
γ-TiPbipy	10.0 ± 0.2	−11.6 ± 0.1	0.9997	211 ± 3	20.1 ± 0.2
γ-TiPbipyCu	8.2 ± 0.6	−10.0 ± 0.4	0.9943	182 ± 8	18.2 ± 0.8

The associated uncertainty are standard deviations.

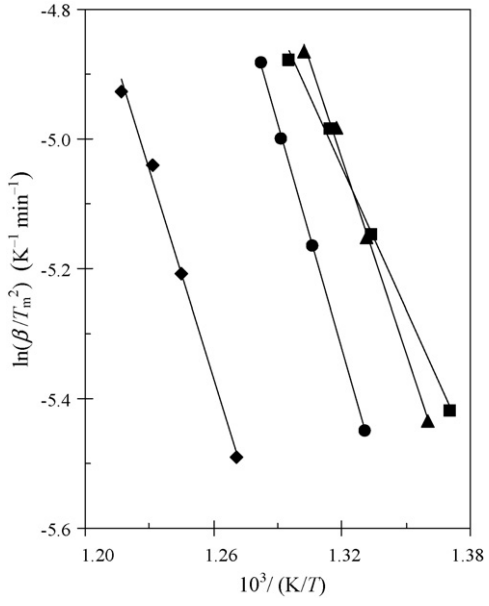

Fig. 9. Kissinger plot for the oxidative decomposition process in γ-ZrPbipy (♦), γ-ZrPbipyCu (■), γ-TiPbipy (●) and γ-TiPbipyCu (▲).

oxidative decomposition processes of γ-ZrPbipy, γ-ZrPbipyCu, γ-TiPbipy and γ-TiPbipyCu the closest matches are found for the models denoted as 13, 6, 4 and 12, respectively, even if these models, except in the case of γ-ZrPbipyCu, do not show unexpectedly the best linear fit of Eq. (8). The corresponding activation energies obtained by the CR method for these above-mentioned models (Tables 6 and 7) are 192.6, 143.9, 291.7 and 242.6 kJ mol^{-1} for γ-ZrPbipy, γ-ZrPbipyCu, γ-TiPbipy and γ-TiPbipyCu, respectively. It is interesting to note that these E values do not differ significantly from the corresponding mean E values selected using the isoconversional OFW method in the range $\alpha \leq 0.7$.

Finally, the Arrhenius parameters obtained by the Kissinger method for the oxidative decomposition step as well as the corresponding rate constants derived using the Arrhenius equation for the intercalation materials containing bipy were compared in Table 8 with the corresponding values for the intercalation materials containing 1,10-phenanthroline [10] and 2,9-dimethyl-1,10-phenanthroline [11]. As far as the bipy and bipyCu intercalation materials are concerned, being activation energies, pre-exponential factors and decomposition tempera-

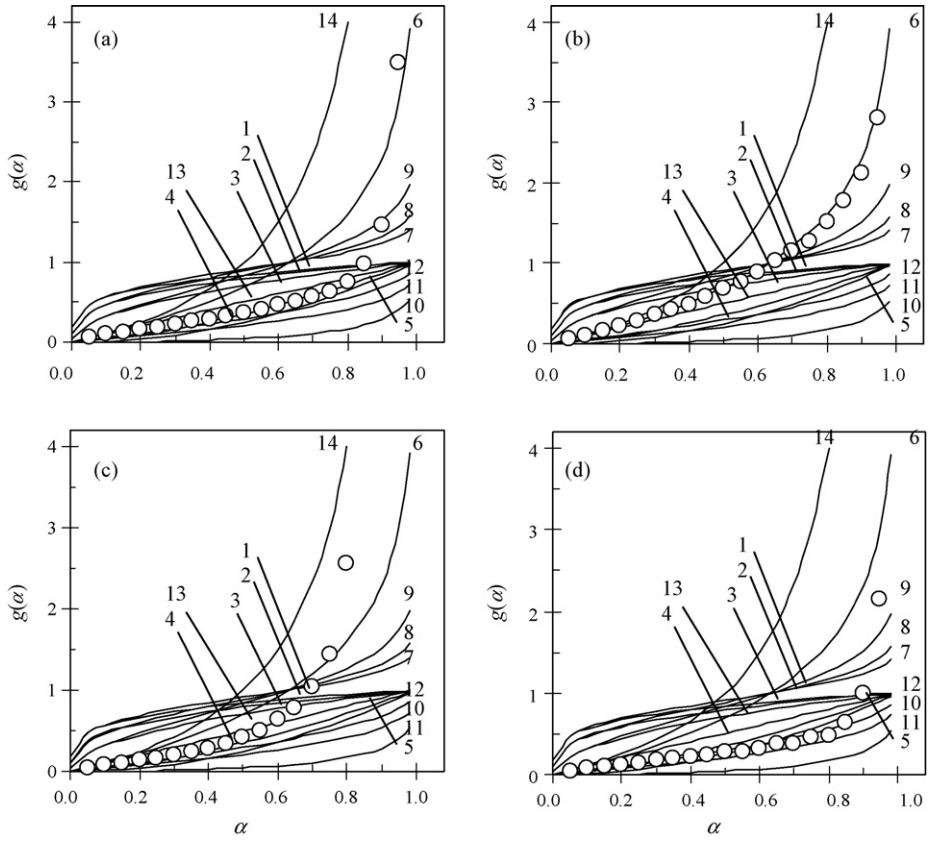

Fig. 10. Conversion dependence of $g(\alpha)$ for the model functions listed in Table 1 (—) and for the experimental data (◯) related to oxidative decomposition of (a) γ-ZrPbipy, (b) γ-ZrPbipyCu, (c) γ-TiPbipy and (d) γ-TiPbipyCu.

tures of decomposition for intercalation bipyCu materials lower than those of the corresponding intercalation bipy materials (Table 8), the material having the highest kinetic stability must be selected only taking into account the only suitable kinetic stability (lability) parameter, which is the rate constant at fixed temperature ($k(\langle T \rangle)$). Thus, a comparison of these values in Table 8 reveals that both the bipyCu intercalation materials show a destabilizing effect with respect to the corresponding bipy intercalation materials (negligible difference in the oxidative decomposition temperatures, but a significant difference in the rate constant values: at least one order of magnitude). In addition, the intercalation materials containing the most hindered ligand (2,9-dimethyl-1,10-phenanthroline), except for the γ-TiPL materials where no significant differences were observed among

Table 6
Arrhenius parameters related to oxidative decomposition of γ-ZrPbipy and γ-ZrPbipyCu materials at 8 K min^{-1} obtained by the Coats–Redfern method for the most commonly used model functions

N	γ-ZrPbipy			γ-ZrPbipyCu		
	E (kJ mol^{-1})	ln(A min^{-1})	R^2	E (kJ mol^{-1})	ln(A min^{-1})	R^2
1	50.2	4.9	0.9625	18.2	0.4	0.9331
2	71.4	8.2	0.9671	28.4	1.8	0.9513
3	113.7	14.9	0.9710	48.8	5.1	0.9633
4	368.0	53.1	0.9752	171.2	24.8	0.9737
5	495.1	71.2	0.9757	232.4	34.3	0.9747
6	311.6	44.8	0.9981[a]	143.9	21.1	0.9965[a]
7	67.9	7.8	0.9974[a]	26.7	1.7	0.9931[a]
8	94.9	12.1	0.9977[a]	39.7	3.8	0.9946[a]
9	149.1	20.4	0.9979[a]	65.8	8.2	0.9957[a]
10	156.1	21.1	0.9727	69.2	8.5	0.9677
11	71.4	8.2	0.9671	28.4	1.8	0.9513
12	273.6	38.2	0.9899	125.7	17.2	0.9884
13	192.6	17.4	0.9742	90.8	15.9	0.9715
14	403.8	59.2	0.9926	188.0	28.8	0.9885

[a] Statistically equivalent models.

Table 7
Arrhenius parameters related to oxidative decomposition of γ-TiPbipy and γ-TiPbipyCu materials at 8 K min^{-1} obtained by the Coats–Redfern method for the most commonly used model functions

N	γ-TiPbipy			γ-TiPbipyCu		
	E (kJ mol^{-1})	ln(A min^{-1})	R^2	E (kJ mol^{-1})	ln(A min^{-1})	R^2
1	37.7	3.1	0.8499	43.6	4.3	0.9043
2	54.7	5.8	0.8704	62.3	7.4	0.9162
3	88.5	11.2	0.8872	99.8	13.5	0.9262
4	291.7	42.4	0.9052	324.9	48.9	0.9370
5	393.3	57.7	0.9072	437.5	66.3	0.9382
6	251.4	36.9	0.9632	278.0	42.2	0.9808
7	53.0	5.7	0.9482	60.0	7.2	0.9738
8	75.1	9.3	0.9540	84.2	11.2	0.9765
9	119.2	16.3	0.9590	132.7	19.0	0.9788
10	122.4	16.5	0.8945	137.3	19.5	0.9305
11	54.7	5.8	0.8704	62.3	7.4	0.9162
12	218.4	30.8	0.9356	242.6	35.6	0.9610
13	127.7	16.9	0.9011	121.2	17.0	0.9345
14	332.0	49.9	0.9936[a]	364.4	56.4	0.9978[a]

[a] Best linear fitting model.

Table 8
Comparison of Arrhenius parameters obtained by the Kissinger method for the oxidative decomposition step of the intercalation materials containing different heterocyclic compounds as ligand

Material	L	E (kJ mol^{-1})	ln(A min^{-1})	$\langle T\rangle$[d] (K)	$k(\langle T\rangle)$[d] (10^{-4} min^{-1})
γ-ZrPL	phen[a]	192 ± 5	17.5 ± 0.7	810	0.17
	dmp[b]	182	19.8	680	0.043
	bipy[c]	194 ± 11	18.1 ± 1.0	806	0.20
γ-ZrPLCu	phen[a]	180 ± 4	17.9 ± 0.6	749	0.16
	dmp[b]	139	15.3	615	0.071
	bipy[c]	133 ± 6	14.3 ± 0.6	753	9.52
γ-TiPL	phen[a]	206 ± 7	19.8 ± 0.9	776	0.053
	dmp[b]	185	20.4	673	0.032
	bipy[c]	211 ± 3	20.1 ± 0.2	768	0.024
γ-TiPLCu	phen[a]	165 ± 4	16.6 ± 0.5	754	0.63
	dmp[b]	138	16.3	573	0.032
	bipy[c]	182 ± 8	18.2 ± 0.8	753	0.19

[a] phen = 1,10-phenanthroline [10].
[b] dmp = 2,9-dimethyl-1,10-phenanthroline [11].
[c] This study.
[d] $\langle T\rangle$ = average of the experimental temperature range considered.

the $k(\langle T\rangle)$ values calculated, usually show the higher kinetic stability effect. This results are mainly due to the lower values of decomposition temperature ($\langle T\rangle$) selected for the decomposition of dmp in the intercalation materials considered (Table 8), regardless the values of E and ln A.

5. Conclusions

Taking into account all the presented results, the following remarks can be drawn:

(i) Vaporization of bipy is described by a single step of mass loss with negligible change in E values, which agree quite well with the vaporization enthalpy derived from DSC measurements.
(ii) The oxidative decomposition of bipy practically occurs in only one step for all the intercalation compounds examined. As far as the oxidative decomposition of bipy is concerned, a destabilizing effect is shown by the bipyCu intercalation materials with respect to the corresponding bipy intercalation materials (comparable oxidative decomposition temperatures, but at least one order of magnitude between the rate constant values). The formation *in situ* of bipyCu complex, between the layers of these materials significantly increases its thermal stability (thermal oxidative decomposition does not occur up to 673 K) and occurs in only one step.
(iii) Activation energies determined by the OFW method do not depend significantly on the degree of conversion for $\alpha \leq 0.7$. Therefore, it was possible to reconstruct the model function $g(\alpha)$ for vaporization of pure bipy and oxidative decomposition concerning the intercalation compounds examined even if sometimes more functions seem to show equivalent linear fit of the model-fitting equation (CR

method). These E values do not differ significantly from the corresponding mean E values selected using the isoconversional OFW method in the range $\alpha \leq 0.7$.

(iv) By comparing the kinetic results presented here with those of the previous our studies on the intercalation materials containing 1,10-phenanthroline and 2,9-dimethyl-1,10-phenanthroline it was shown that a comparable stabilizing effect is shown in all the three intercalation γ-TiPL materials due to a sort of compensation effect between the enthalpic contribution of activation energy and the entropic contribution of pre-exponential factor. For all the other intercalation materials the lower temperature regions in which the decomposition of dmp occurs with respect to those (comparable) of phen and bipy is the main parameter influencing the kinetic stability.

Acknowledgements

The authors greatly acknowledge the Italian C.N.R. and M.I.U.R. for their financial supports.

References

[1] A. Clearfield, G.D. Smith, Inorg. Chem. 8 (1969) 431.
[2] S. Yamanaka, M. Tanaka, J. Inorg. Nucl. Chem. 41 (1979) 45.
[3] S. Allulli, C. Ferragina, A. La Ginestra, M.A. Massucci, M. Tomassini, J. Inorg. Nucl. Chem. 39 (1977) 1043.
[4] A. Clearfield, J.M. Kalnins, J. Inorg. Nucl. Chem. 38 (1976) 849.
[5] A. Clearfield, in: A. Clearfield (Ed.), Inorganic Ion-Exchange Materials, CRC Press, Boca Raton, FL, 1982, p. 20.
[6] C. Ferragina, M.A. Massucci, A. La Ginestra, P. Patrono, A.A.G. Tomlinson, J. Chem. Soc., Chem. Commun. 15 (1984) 1024.
[7] C. Ferragina, M.A. Massucci, A. La Ginestra, P. Patrono, J. Chem. Soc., Dalton Trans. 2 (1986) 265.
[8] C. Ferragina, P. Caffarelli, R. Di Rocco, J. Therm. Anal. Cal. 63 (2001) 709.
[9] C. Ferragina, R. Di Rocco, L. Petrilli, Thermochim. Acta 409 (2004) 177.
[10] S. Vecchio, R. Di Rocco, C. Ferragina, S. Materazzi, Thermochim. Acta 435 (2005) 181.
[11] S. Vecchio, R. Di Rocco, C. Ferragina, Thermochim. Acta 453 (2007) 105.
[12] C. Ferragina, A. La Ginestra, M.A. Massucci, P. Patrono, P. Giannoccaro, F. Nobile, G. Moro, J. Mol. Catal. 53 (1989) 349.
[13] M. Lenarda, R.L. Ganzerla, R. Zanoni, J. Mol. Catal. 78 (1993) 339.
[14] P. Giannoccaro, S. Doronzo, C. Ferragina, in: H.U. Blaser, A. Baiker, R. Prins (Eds.), Heterogeneous Catalysis and Fine Chemicals, vol. IV, Elsevier Science, New York, 1997, p. 633.
[15] C. Ferragina, M.A. Massucci, A.A.G. Tomlinson, J. Chem. Soc., Dalton Trans. (1990) 1191.
[16] C. Ferragina, A. La Ginestra, M.A. Massucci, P. Cafarelli, P. Patrono, A.A.G. Tomlinson, in: P.A. Williams, M.J. Hudson (Eds.), Recent Developments in Ion Exchange, vol. 2, Elsevier Applied Science, London/New York, 1990, p. 103.
[17] M. Arfelli, G. Mattogno, C. Ferragina, M.A. Massucci, J. Incl. Phenom. Mol. Recognit. 11 (1991) 15.
[18] G. Alberti, U. Costantino, E. Torracca, J. Inorg. Nucl. Chem. 28 (1966) 225.
[19] R. Hultgren, P.D. Desai, D.T. Hawkins, M. Gleiser, K.K. Kelley, D.D. Wagman, Selected Values of the Thermodynamic Properties of the Element, American Society for Metals, Metals Park, OH, 1973.
[20] X. Gao, D. Chen, D. Dollimore, Thermochim. Acta 223 (1993) 75.
[21] A.K. Galwey, M.E. Brown, Thermal Decomposition of Ionic Solids, Elsevier, Amsterdam, 1999.
[22] S. Vyazovkin, C.A. Wight, Annu. Rev. Phys. Chem. 48 (1997) 125.
[23] J.H. Flynn, L.A. Wall, J. Polym. Sci. B: Polym. Lett. 4 (1966) 323.
[24] T. Ozawa, Bull. Chem. Soc. Jpn. 38 (1965) 1881.
[25] C.D. Doyle, J. Appl. Polym. Sci. 6 (1962) 639.
[26] H.E. Kissinger, Anal. Chem. 29 (1957) 1702.
[27] S. Vyazovkin, C.A. Wight, J. Phys. Chem. A 101 (1997) 5653.
[28] A.W. Coats, J.P. Redfern, Nature 201 (1964) 68.
[29] S. Vyazovkin, Int. J. Chem. Kinet. 28 (1996) 95.
[30] C. Ferragina, P. Caffarelli, R. Di Rocco, Mater. Res. Bull. 33 (1998) 305.
[31] D. Dollimore, Thermochim. Acta 340–341 (1999) 19.
[32] P. Aggarwal, S. Pereira, D. Dollimore, Thermochim. Acta 324 (1998) 9.
[33] L. Shen, K.S. Alexander, Thermochim. Acta 340–341 (1999) 271.